Analytical solutions for peak and residual uplift resistance of pipelines

J.F. (Derick) Nixon
Nixon Geotech Ltd. Calgary AB, Canada
James M. Oswell
Naviq Consulting Inc. Calgary, AB, Canada

ABSTRACT
Cold pipelines that traverse unfrozen (non permafrost) terrain are susceptible to frost heave. The stresses experienced by the pipeline are partially a function of the strength of the soil on the non heaving side of the frozen-unfrozen interface. In this paper, three analytical solutions are proposed to estimate the soil uplift resistance by considering the pipeline and soil to act similar to a strip footing, a punching shear failure, and by considering the formation of horizontal crack emanating from the spring line of the pipe.

The study found that the peak uplift resistance and the residual uplift resistance were generally independent and controlled by different factors. The peak resistance is related directly to pipe diameter, and less strongly dependent on springline depth. It is also strongly dependent on soil temperature. In contrast, the residual uplift resistance is strongly dependent on burial depth, weakly dependent on pipe displacement rate and also on soil temperature.

RÉSUMÉ
Les pipelines froids qui traversent des terrains non-gelés (non-pergélisol) sont susceptibles de rencontrer des soulèvements du au gel. Les stress subit par les pipelines dépendent partiellement de la résistance du sol sur le côté non soulevé de l'interface congelé-dégelé. Dans cet article, trois solutions analytiques sont proposées pour estimer la résistance au soulèvement du sol en considérant que le pipeline et le sol ont un comportement similaire à une semelle filante, un échec poinçonnement, et en considérant la formation de fissures horizontales émanant de la gamme de printemps de la conduite.

L'étude a révélé que la résistance au soulèvement maximal et la résistance au soulèvement résiduel sont généralement indépendants et contrôlées par différents facteurs. La résistance maximale est directement liée au diamètre du conduit, et moins fortement dépendant de la profondeur en ligne au printemps. Elle est également fortement dépendante de la température du sol. En revanche, la résistance au soulèvement résiduel est fortement dépendante de la profondeur d'enfouissement, faiblement dépendante au taux de déplacement de la conduite et à la température du sol.

1 INTRODUCTION

When a cold pipeline crosses a thermal or textural transition, one side of the interface may heave upwards over time because of ice lensing in the frost susceptible soil. This upward heave is resisted by the pipe embedded in stable frozen soil, as shown in Figure 1.

To a large extent the magnitude of the frozen soil resistance controls the bending strains in the buried pipe, and therefore it is important to have a clear understanding of the factors influencing uplift resistance.

If a unit length of buried pipe is displaced upwards at a given rate, the load on the pipe increases steadily to a peak load, and then may decay towards a post-peak or "residual" load. See insert in Figure 1.

There have been several laboratory scale tests undertaken to measure peak and residual uplift resistance (Nixon and Hazen, 1993; Nixon, 1998). In addition, one intermediate scale test was carried out by Foriero and Ladanyi (1994) at the Caen, France test basin. When scaling up to a full scale pipe, it is very important to understand the controlling variables. This issue is explored in the present paper.

2 PEAK UPLIFT RESISTANCE

It has been repeatedly observed in both full scale field uplift events and laboratory scale tests that a crack forms vertically over the pipe through the soil cover and further soil cracks propagate horizontally or sub vertically from the pipe springline.

There are a number of possible approaches to obtaining an analytical solution for peak uplift resistance in frozen soil. The first approach is to assume that two vertical shear planes form over the pipe, as shown in Figure 2. For model A, the peak resistance can be estimated very simply from

$$P_U = \gamma\, d\, H + 2\, C_u\, H \qquad [1]$$

where C_u = frozen soil cohesion and is equal to one-half the compressive strength, σ_c . Therefore

$$P_U = \gamma\, d\, H + \sigma_c\, H \qquad [2]$$

This resistance mechanism is more likely to be appropriate for shallow cover depths.

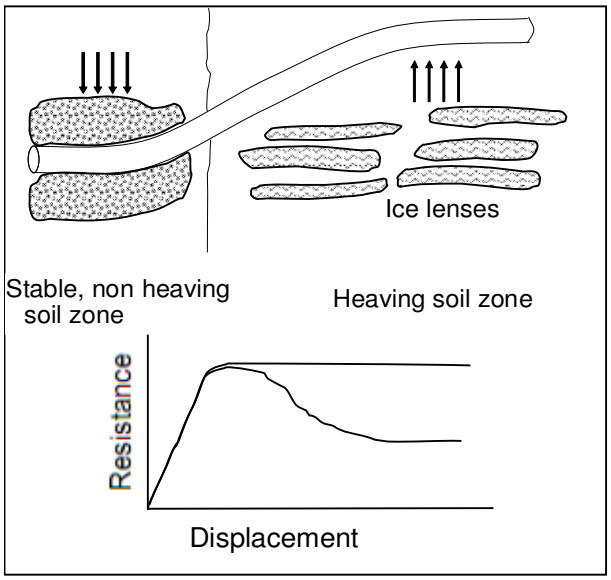

Figure 1. Schematic of frost heaving under pipeline problem (not to scale).

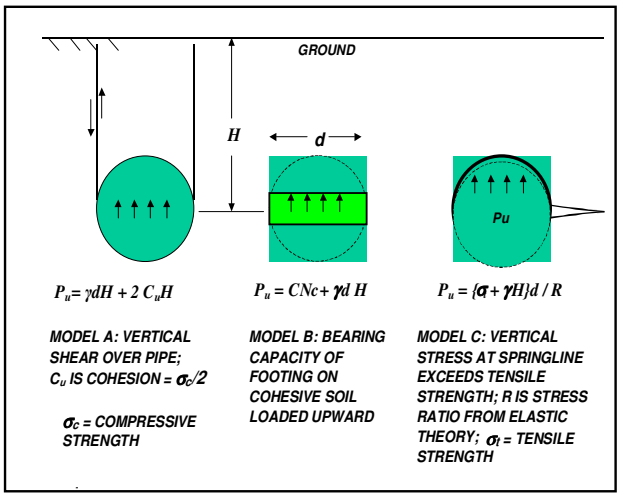

Figure 2. Schematic of three uplift models for peak resistance.

A second approach (Model B in Figure 2) is to assume the pipe acts as a strip footing loaded vertically upwards, and the standard bearing capacity equation would apply, i.e.

$$P_U = N_c\, C_u\, d + \gamma\, d\, H \qquad [3]$$

where N_c is a bearing capacity factor equal to about 6 for a rectangular strip footing.

So
$$P_u = 3\,\sigma_c\, d + \gamma\, d\, H \qquad [4]$$

This mechanism is more likely to be relevant for a very deeply buried footing (pipe).

A third method (Model C in Figure 2) would be to calculate the vertical stress at the pipe springline, and compare this with the tensile strength of the frozen soil. Once the vertical stress exceeds the tensile strength, it can be assumed that the soil will tend to crack horizontally, and peak uplift resistance will be imminent. There is no simple elastic solution for a semi-circular surface subjected to a uniform vertical stress. A common way to obtain a solution to such a problem in solid mechanics is to superimpose a series of point loading to obtain the integrated vertical stress at the point of interest in the solid medium. Integration of Mindlin's vertical point load equation (Poulos and Davis, 1971) for the geometry shown in Figure 2, Model C yields the desired solution.

A unit stress is applied upwards to the inside of semi-circular surface, and the surface is divided into thousands of small equivalent point loads. The solution is evaluated for several different cover depths; the normalized results are given on Figure 3.

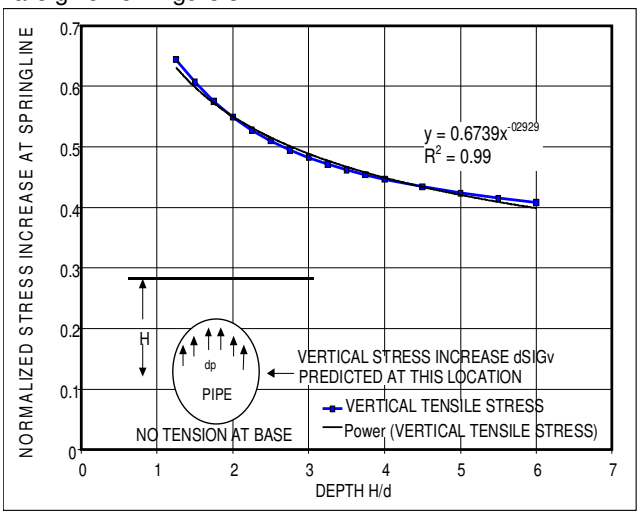

Figure 3. Vertical stress as a function of normalized pipe depth for Model C.

If the ratio $d\sigma_v$ / dp is labelled R, then the vertical uplift resistance, P_U, can be related to the tensile stress increase at the pipe springline as

$$d\sigma_t = R\, P_U / d \qquad [5]$$

If the stress increase at the springline exceeds $\sigma_t + \gamma H$ then it can be assumed the peak resistance has been reached. This equality is written as:

$$R\, P_U / d = \sigma_t + \gamma H \qquad [6]$$

or
$$P_U = \{\sigma_t + \gamma\, H\}\, d / R$$

By selecting tensile and compressive strength – temperature relationships for time to failure of a few days or so, each of the above three models can be compared for different soil temperatures and cover depths. The chosen strength relationships (see Figure 4) are considered reasonable for a clayey soil such as Calgary silty clay tested by Nixon (1998), but would be significantly higher for a silty soil. The peak uplift resistance for the three models are compared in Figure 5 for a soil temperature of -5°C.

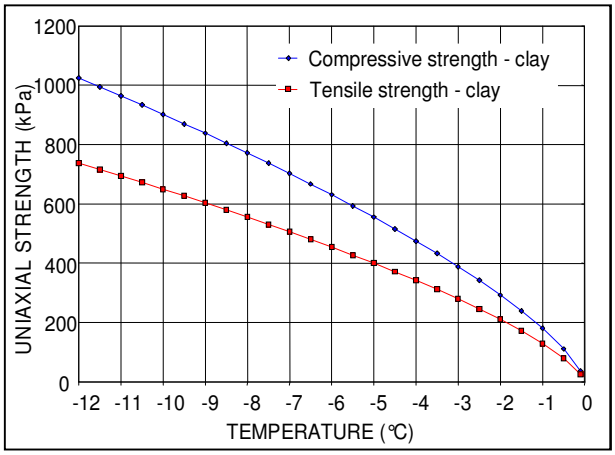

Figure 4. Compressive and tensile strength relationship with temperature (from Nixon, 1998).

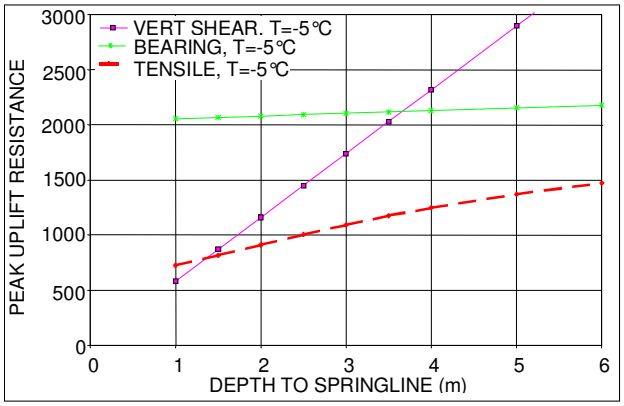

Figure 5. Predicted peak uplift resistance for soil at -5 °C for soil models presented in Figure 2.

From Figure 5, it is seen that model A, (vertical shear planes over the pipe), only governs for a very small range of cover depths at the very low end of the cover depth scale. Model B, the bearing capacity of a strip footing scenario will likely never govern the peak uplift, at least for these rates of loading. Model C on the other hand (soil tensile strength exceeded) governs for most of the practical range of cover depths.

3 RESIDUAL UPLIFT RESISTANCE

3.1 General

It had been repeatedly observed in laboratory scale tests and in operating pipelines subject to uplift that a crack forms vertically over the pipe at or near the point of peak resistance, and further soil cracks propagate out horizontally or sub vertically from the pipe springline.

One approach to considering the soil load reduction resulting from the crack formation would be to assume the crack pattern as described above has already taken place, and analyze the residual frozen soil resistance as the sum of the flexural resistance of two frozen cantilevered “beams” and the static weight of the beams on either side of the pipe, as illustrated in Figure 6. This can be done using a relatively straightforward analytical derivation with no numerical analysis required, and results provided in spreadsheet form so that the sensitivity to the important input variables can be quickly explored. The residual resistance for this case will be essentially unrelated to any other analysis for peak uplift resistance. The analysis should indicate the important variables, both geometric and soil properties that will control the residual uplift resistance.

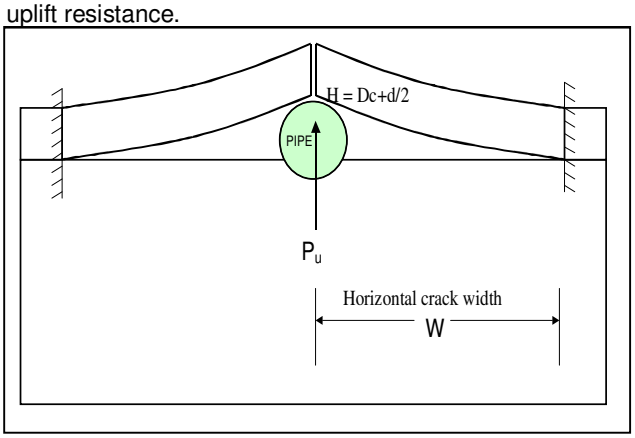

Figure 6. Idealized soil geometry for residual uplift resistance.

Bearing in mind that a much greater proportion of a frost heaving pipe is subject to residual resistance, and the length of pipe experiencing peak resistance is relatively limited, the results of the analysis may have significant implications on the pipe structural analysis for frost heave.

A solution is obtained for the secondary creep of the frozen soil adjacent to the pipe. Soil cracks are assumed to form vertically over the pipe, and horizontally from the pipe springline, thereby dividing the frozen soil region over the pipe into two frozen soil cantilevers. Because of horizontal stratification in the soil, horizontal ice lensing and previous advances of the active layer, the soil may crack preferentially in a horizontal direction, for at least some distance out from the pipe springline.

The simplest creep formulation for icy frozen soils uses the secondary creep law

$$\dot{\varepsilon} = B\sigma^3 \qquad [7]$$

where $\dot{\varepsilon}$ is the uniaxial steady creep rate,

B is the temperature dependent creep coefficient in units of $kPa^{-3}\ yr^{-1}$

σ is the uniaxial applied stress

Figure 7 presents a summary for the creep coefficient for ice and icy soils showing the temperature dependency for B. A lower bound relationship was used for this study, as this will provide conservative (higher) values for icy soils, and is $B = 3x10\text{-}8/(1\text{-}T)^{1.5}$.

If the total uplift load is P, then the applied moment on each frozen beam is

$$M = \frac{Px}{2} \qquad [8]$$

where x is the distance from the pipe center-line along the crack width.

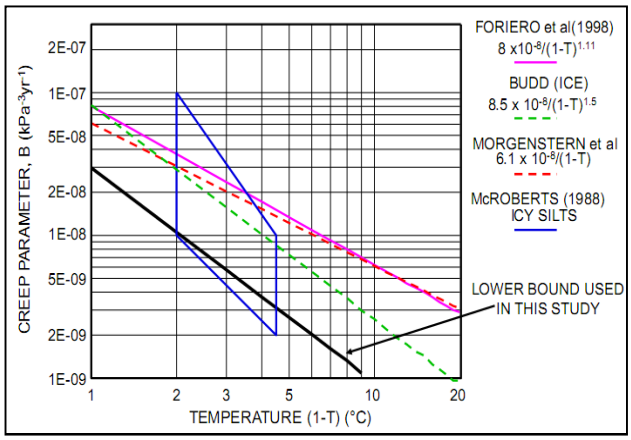

Figure 7. Creep relationship for ice and icy permafrost soils.

The moment resistance of the frozen beam is calculated assuming compressive and tensile creep properties are the same, and the neutral axis for the beam remains at the mid-height of the beam. Figure 8 illustrates the strain rate and stress distribution vertically through the beam.

Figure 8 shows a linear strain rate distribution through the beam, that varies from zero at the neutral axis (y=0), to the maximum fibre strain rate E_c at y = H/2. Further, in the same way as used for linear elastic beam theory, the maximum fibre strain is related to the radius of curvature of the beam, and the second derivative of the beam displacement as shown in the beam. However, note that the following obtains a solution for steady displacement rate, y, and not beam displacement itself.

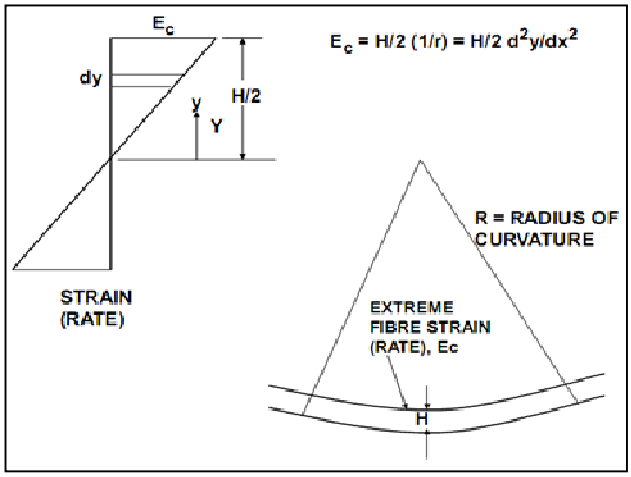

Figure 8. Stress distribution and strain rate within a beam.

The strain rate varies linearly through the beam as

$$\dot{E} = \frac{E_c y}{\left(\frac{H}{2}\right)} \qquad [9]$$

Using the secondary flow law, the stress in each beam fibre is then

$$\sigma = \left[\frac{E_c y}{BH/2}\right]^{1/3} \qquad [10]$$

Integrating the stresses through the beam, the moment resistance of the beam is

$$M = 2\int_0^{H/2} \sigma y L dy \qquad [11]$$

where L is the dimension parallel to the pipe (into the plane of Figure 8).

Note that the above assumes the same creep properties in tension and compression. After integration, we obtain

$$\frac{Px}{2} = \left[\frac{6L}{7}\frac{2E_c}{BH}\right]^{1/3}\frac{H^{7/3}}{2} \qquad [12]$$

Re-arranging equation 12, and using the above relating beam curvature to extreme fibre strain, we obtain a partial differential equation for displacement rate, y, with distance along the beam, x:

$$\frac{d^2y}{dx^2} = \left[\frac{7}{6L}\frac{P}{2}x\right]^3 \frac{B}{(H/2)^7} \qquad [13]$$

Integrating twice with distance, x, and using the boundary conditions y=0 at x=W, and dy/dx=0 at x=W, we finally obtain an expression for P/L, the residual resistance per unit distance along the length of pipeline

$$\frac{P}{L} = \frac{12}{7}\left[\frac{Y_o\left(\frac{H}{2}\right)^7}{\frac{BW^5}{5}}\right]^{1/3} + 2\gamma HW \qquad [14]$$

where Y_o is the applied displacement rate at the pipe location, x=0.

The second term has been added to account for the self weight of the beam segments on both sides of the pipe. There is some uncertainty here as the entire gravity load of the beams is assumed to be borne by the pipe. Simple statics would suggest that one half of the reaction load to the beam weight should be borne by the soil at the end of the beam, x=W. The distribution of the reaction load is not known, and for the moment it is conservatively assumed to be borne by the pipe.

At this stage of the analysis the width of the horizontal soil crack is not known. However, when the total residual

uplift load is plotted with crack width, there is always a minimum value some distance out from the pipe.

An expression for the crack width where P/L is a minimum can be obtained by differentiating equation 14, and setting the result equal to zero, yielding

$$W_{cr} = \left\{ \frac{2\,\gamma\,H}{\frac{4}{7}(5)^{4/3}} \left[\frac{Y_o(\frac{H}{2})^7}{B} \right]^{1/3} \right\}^{-3/8} \qquad [15]$$

Examination of equation 15 suggests that the crack width is proportional to about $H^{1/2}$. This minimum also depends on pipe displacement rate. This means that as the crack develops, the residual load will fall (as observed in tests), but will reach some limiting extent, which limits the propagation of the crack.

3.2 Results for full scale pipe

The pipe diameter itself does not appear in the formulation, except in the sense that the depth to springline appears, H = d/2 + D_c (pipe radius plus cover depth).

The total residual resistance is the sum of two components, the flexural resistance of the beams, and the static weight of the soil beams. It is of interest to see how each varies with horizontal crack width, W, as shown in Figure 9 for a specified displacement rate of 0.3 m/year for a nominal pipe depth of 1.5 m.

The flexural resistance decays at almost an inverse square law, whereas the weight component increases linearly with crack width. Figure 10 presents the residual uplift resistance for a range of displacement rates. It is observed that at some crack width, there is always a minimum value depending on the key geometric properties.

The minimum residual uplift resistance can be plotted with applied displacement rate, and the results are related to the applied displacement rate raised to the power of 8, as shown on Figure 11.

Even though the creep law (equation 6) states that strain rate is related to stress raised to the power of 3, the final residual uplift load is related to displacement rate raised to the power of 8.

3.3 Results for laboratory scale model pipes

Using the analytical solution, the following results for the laboratory scale experiment become available (H = 0.21 m), as illustrated in Figure 12.

It is important to note that the analysis suggests that true residual would not be reached in a small uplift box tests until the lateral extent of cracking is of the order of 1.0 m. Thus this may be useful in defining the minimum dimensions of a laboratory scale test cell.

Figure 13 and Figure 14 show the results of the total residual uplift resistance as a function of displacement rate, and the minimum total residual uplift resistance as a function of displacement rate, respectively for the case of H = 0.21 m. The residual uplift resistance is very much lower, but the same trends are apparent at the laboratory scale.

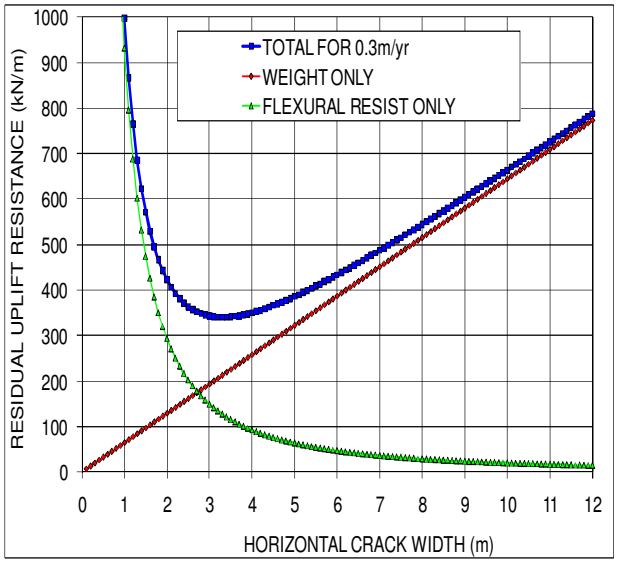

Figure 9. Components of residual uplift resistance for full scale pipes as a function of horizontal crack width. The upward displacement rate is 0.3 m/year.

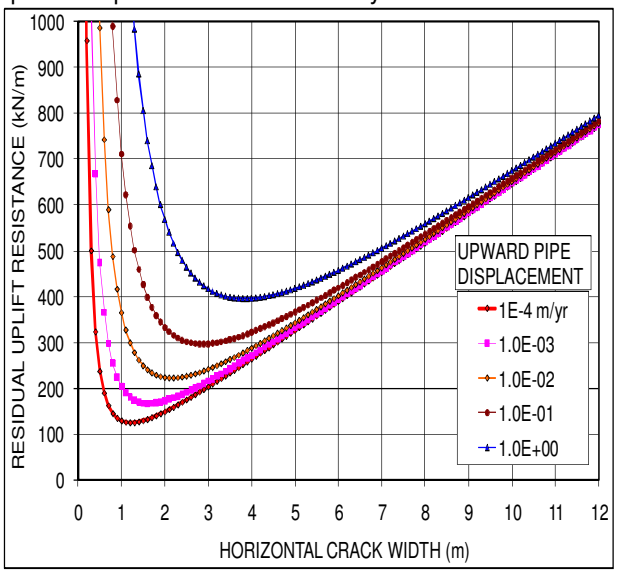

Figure 10. Residual uplift resistance for full scale pipes for a range of displacement rates.

3.4 Cover Depth, Temperature and Crack Width

The closed-form solution can now be used to examine the effects of some important uplift variables. The first of these is the depth to the pipe springline (cover depth plus pipe radius), and this is shown in Figure 15. The residual uplift resistance is dependent on the crack width from the pipe centreline, although the crack width does not need to be determined independently; it is a product of the solution method. Using the expression for W_{cr} derived earlier (equation 15), the relationship for W_{cr} with depth to springline is shown in Figure 16.

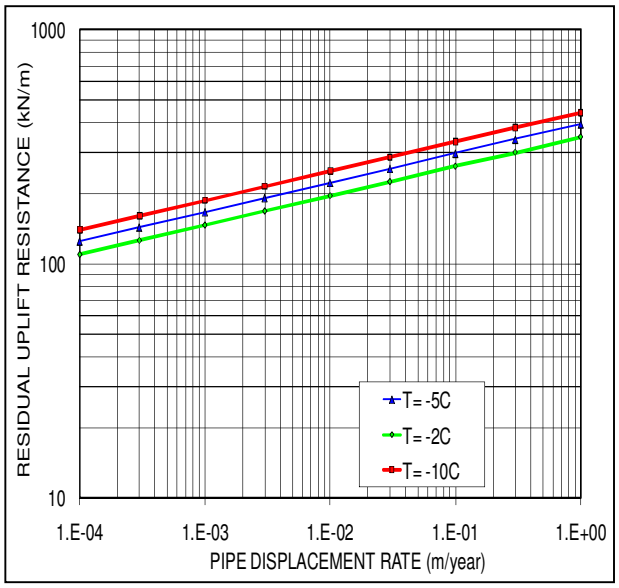

Figure 11. Minimum residual uplift resistance for a full scale pipe as a function of displacement rate (log-log scale).

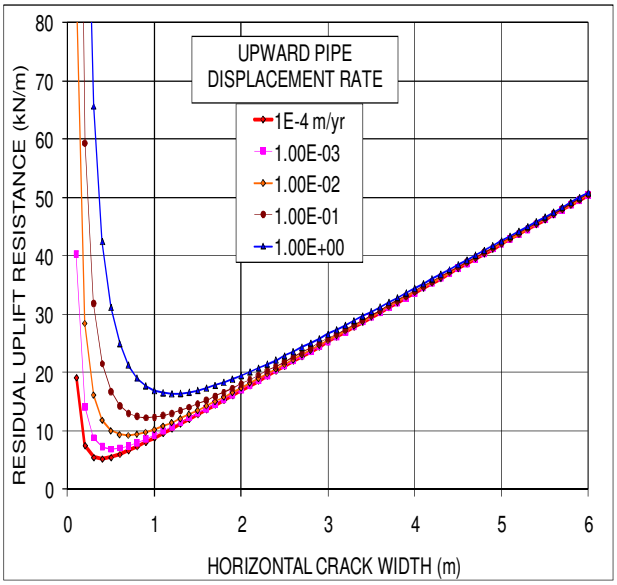

Figure 13. Total residual uplift resistance with a displacement rate for H = 0.21m.

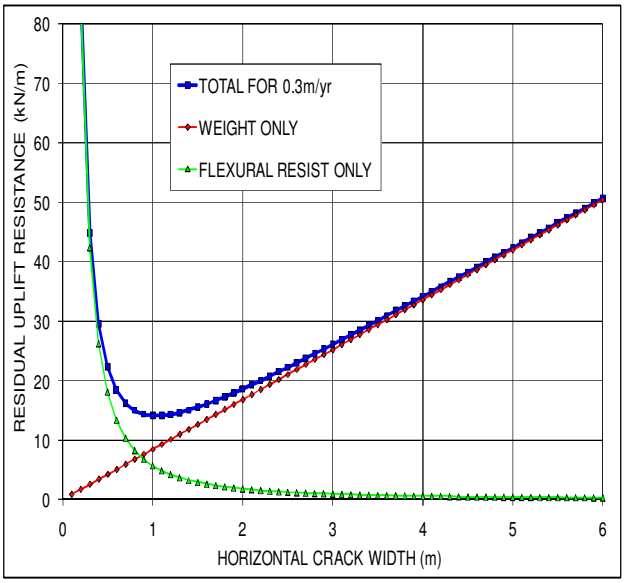

Figure 12. Components of residual uplift resistance for H = 0.21 m. The upward displacement rate is 0.3 m/year.

Soil temperature enters into the analysis through the secondary creep parameter, B. Although B is strongly influenced by temperature, the residual uplift resistance is related to B by the 1/3 power, so the effect of soil temperature is less than might be anticipated, as shown Figure 17.

Soil density is also a variable, but has a smaller possible range than other inputs, and therefore a limited effect on the results. It is found that all possible results from this residual uplift analysis can be predicted exactly by the following function

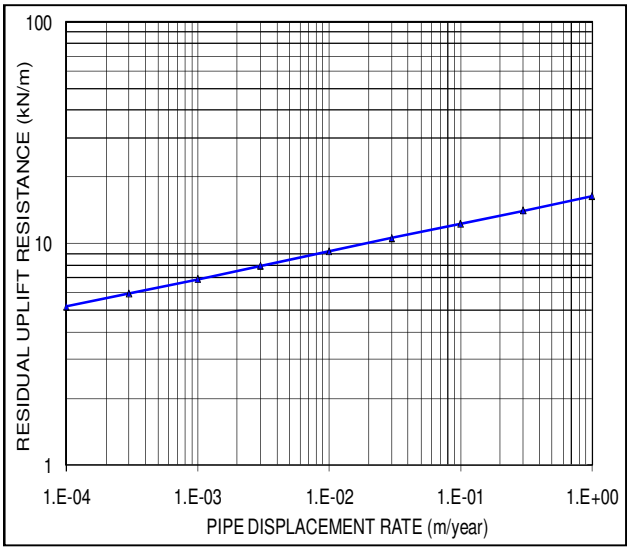

Figure 14. Minimum residual uplift resistance as a function of displacement rate (log-log scale) for H = 0.21 m.

$$P_r = 138.26 H^{1.5} (1-T)^{0.1875} \dot{S}^{0.125} \quad [16]$$

where P_r is in kN/m, T in ℃, H is the depth to the springline in metres, and $\dot{S}$ is given in m/year.

3.5 Limits to Residual Uplift Resistance

In practice, an upper limit could be placed on the residual resistance, where it cannot be greater than the peak resistance. This may be required at greater cover depths, where the residual resistance increases more quickly with depth than the peak resistance. Alternatively,

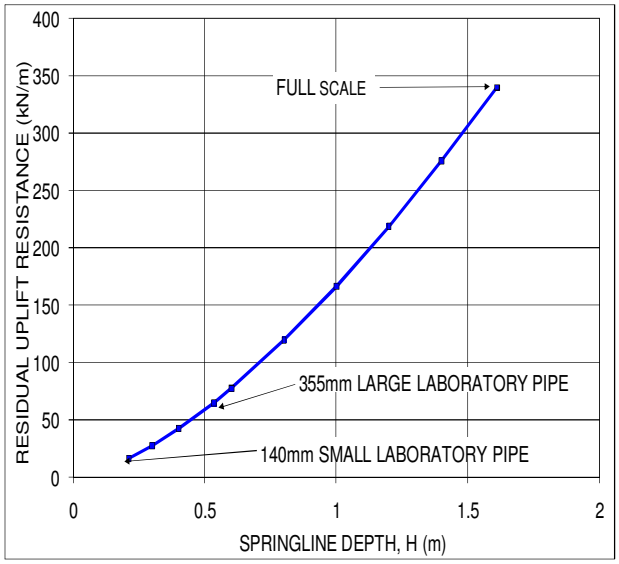

Figure 15. Effect of pipe springline depth on residual uplift resistance. The upward displacement rate is 0.3 m/year.

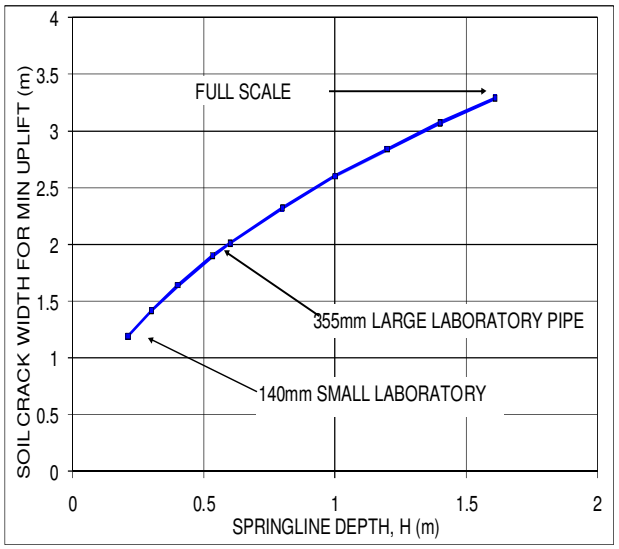

Figure 16. Predicted effect of horizontal soil crack width as a function of springline depth. The upward displacement rate is 0.3 m/year.

the uplift resistance can be allowed to increase gradually towards a higher residual value.

Some of the main observations made based on the above analysis include

- When the weight and flexural resistance of the frozen soil beams over the pipe are considered, there is always a horizontal crack width for which the residual uplift load is a minimum. It is suggested that this may be the maximum extent to which the soil will crack horizontally.
- The residual uplift resistance increases approximately as the depth to pipe springline raised to a power of 1.5. While pipe diameter does not appear directly in the formulation, the cover depth over the pipe will have a very strong effect on the predicted residual uplift.
- The residual uplift resistance is weakly dependent on pipe displacement rate. Even though the basic soil flow law relates strain rate to σ^3, the analytical solution predicts that the pipe displacement rate is related to residual load raised to the power of eight.
- The residual uplift resistance is predicted to be only weakly dependent on temperature. This is in contrast to the peak resistance, where a strong dependence on temperature is anticipated.
- A single exact function has been provided to give the residual uplift as a function of the three important variables, H, T and $\dot{S}$.
- The residual uplift resistance may be controlled by different geometric variables than the peak resistance, and so the ratio between peak and residual resistance may be quite different as the cover depth is increased, for example.

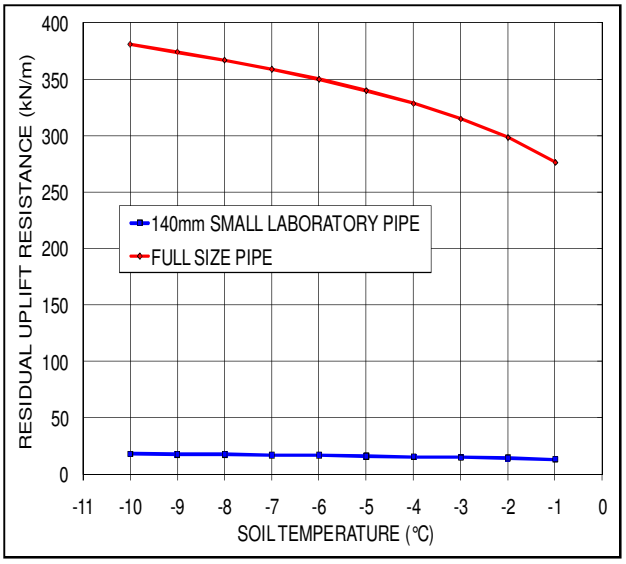

Figure 17. Effect of temperature on the residual uplift resistance.

The residual uplift resistance analysis procedure has been advanced for discussion purposes, and no effort has been made yet to validate or calibrate the model with observed physical tests.

4 PEAK TO RESIDUAL UPLIFT RESISTANCE

Previous correlations (Liu, Crooks, Nixon and Zhou, 2004) relate the residual resistance to the peak resistance by a fixed ratio of 0.5, based on reviewing results from many small scale lab tests, done mostly at cover depth to pipe diameter ratios of 1.0.

The above analysis for peak uplift suggests a direct relationship with pipe diameter, and a weaker dependence on depth to springline, H. Figure 18 compares the relationships with springline depth for a soil

temperature of –5 ℃ for two pipe diameters. Also shown is the residual uplift resistance relationship from Figure 15.

For a soil temperature at –5℃, the peak is greater than residual up to a springline depth of about 3.8 m, after which the residual is greater than peak. In reality, it is likely that there would be no drop-off in load from the peak load, and the P-y curve would become near-horizontal after the initial peak was reached. For the pipe at –2 ℃, (data not shown) the same situation occurs at a smaller springline depth of about 2.5 m. This occurs because the predicted residual resistance is much less sensitive to temperature, whereas the peak resistance is more temperature sensitive through the tensile strength – temperature relationship.

The above comparisons between peak and residual show the likely trends in each for greater cover depths that may be encountered at river and highway crossings. The comparisons also illustrate very clearly that residual should not be related to peak resistance using a constant uplift resistance ratio.

Future uplift resistance correlations will need to provide independent correlations for both peak and residual resistance, perhaps using some of the above findings as guidance for empirical correlation development.

Some qualitative support for the effect of cover depth on the transition from peak to residual resistance can be obtained from the previously reported uplift resistance tests (Nixon and Hazen, 1993), as shown in Figure 19. For a cover depth (D_c) of 0.5 times the pipe diameter, the residual resistance falls to a much lower fraction of peak later in the test.

Tests at larger cover depths are needed to confirm these trends with different cover depths. Some of the main observations that can be made based on the above include

- An exact analytical solution is advanced for peak uplift, based on an idealized elastic solution for tensile stresses at the pipe springline adjacent to the pipe.
- When the soil weight and tensile stress at the springline exceed the tensile strength of the soil, it is assumed that peak uplift resistance has been reached.
- The peak resistance is related directly to pipe diameter, and less strongly dependent on springline depth. It should be recalled that residual uplift resistance increases as the power of 1.5 of the depth to pipe springline.
- The peak uplift resistance is only related to pipe displacement rate through the choice of the tensile strength relationship appropriate for the time to failure involved.
- The peak uplift resistance is quite strongly dependent on soil temperature. This is in contrast to the residual resistance, where a weaker dependence on temperature is anticipated.

ACKNOWLEDGEMENTS

The authors would like to acknowledge the contributions of Dr. Joe Zhou of TransCanada Pipelines Limited, John Greenslade of JGG Consulting Ltd., and Beez Hazen of Northern Engineering and Scientific Limited for their input during the course of this work.

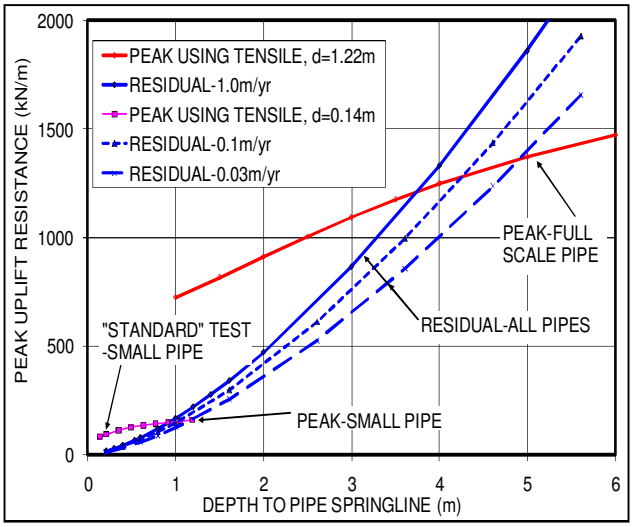

Figure 18. Peak uplift resistance as a function of depth to pipe springline (H) for soil temperature -5℃.

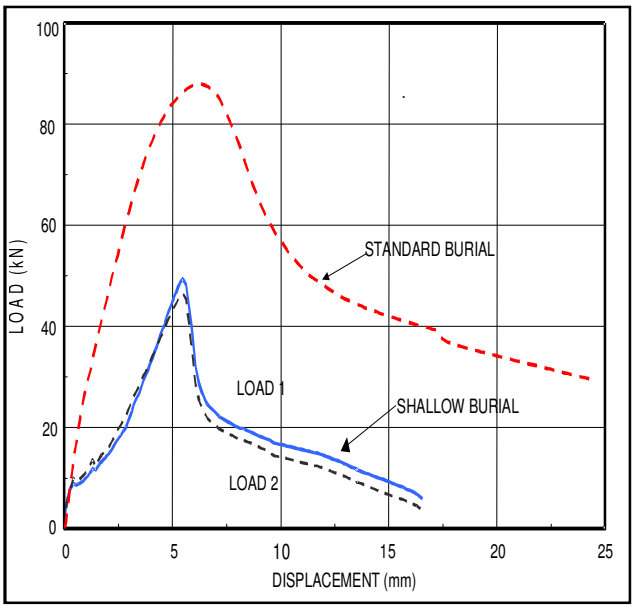

Figure 19. Uplift resistance versus pipe displacement for two burial depths. Pipe diameter is 140 mm; pipe depth is 140 mm and 70 mm; soil temperature is -5 ℃; displacement rate is 1 mm/day.

REFERENCES

ASCE, 1984. *Guidelines for the seismic design of oil and gas pipeline systems*. Committee on Gas and Liquid fuel lifelines. American Society of Civil Engineers, New York, NY.

ASCE, 2001. *Guidelines for the design of buried steel pipe. Appendix B*, America Society of Civil Engineers, New York, NY: 68 – 76.

Budd, W. and Jacka, T. 1989. A review of ice sheet rheology for ice sheet modeling. *Cold Regions Science and Technology*, 16: 107-144.

Foriero, A. and Ladanyi, B. 1994. Pipe uplift resistance in frozen soil and comparison with measurements. *ASCE Journal of Cold Regions Engineering*, 8(3): 93-111.

Liu, B., Crooks, J., Nixon, J., and Zhou, J. 2004. Experimental studies of pipeline uplift resistance in frozen ground. Proceedings *International Pipeline Conference*, Calgary, Canada.

McRoberts, E.C. 1988. Secondary creep interpretations of ice-rich permafrost. Proceedings, *5th International Permafrost Conference*, Trondheim, Norway: 1137-1142.

Morgenstern, N, Roggensack, W., and Weaver, J. 1980. Behaviour of friction pile in ice and ice rich permafrost. *Canadian Geotechnical Journal*, 17(3): 405-415.

Nixon, J. and Hazen, B. 1993. Uplift resistance of pipes in frozen soil. Proceedings. 6th *International Permafrost Conference,* Beijing, China.

Nixon, J.F. 1977. Design Approaches to foundations in permafrost areas. *Canadian Geotechnical Journal*. 14.

Nixon, J. 1994. Role of heave pressure dependency and soil creep in stress analysis for pipeline frost heave. Proceedings, *7th International Cold Regions Specialty Conference*, Edmonton, March 7-9: 397-412.

Nixon J. 1998. Pipe uplift resistance testing in frozen soil. Proceedings *7th International Permafrost Conference*, Yellowknife, NT.

Nixon, J. F. 1992. Seasonal and climate warming effects on pile creep in permafrost. Proceedings, *5th Canadian Permafrost Conference*, Quebec City: 335-340.

Poulos and Davis, 1970. *Elastic solutions in soil mechanics*. McGraw Hill Company, New York, NY: pg. 182.

Poulos and Davis, 1970. *Elastic solutions in soil mechanics*. McGraw Hill Company, New York, NY: pg. 182.

Zhu, Y., and Carbee, D.L. 1987. Tensile strength of frozen silt. *Special Report 87-15*. U.S. Army Corps of Engineers Cold Regions Research and Engineering Laboratory, Hanover, N.H.